Chemical Reactions of Atomic Lithium and Molecular Calcium Monohydride at 1 K

Vijay Singh, Kyle S. Hardman, Naima Tariq, Mei-Ju Lu, Aja Ellis, Muir J. Morrison, and Jonathan D. Weinstein

Phys. Rev. Lett. **108**, 203201 — Published 14 May 2012

DOI: 10.1103/PhysRevLett.108.203201

Chemical Reactions of Li and CaH at 1 Kelvin

Vijay Singh, Kyle S. Hardman, Naima Tariq, Mei-Ju Lu, Aja A. Ellis, Muir J. Morrison, and Jonathan D. Weinstein*
Department of Physics, University of Nevada, Reno NV 89557, USA

Using cryogenic helium buffer-gas cooling, we have prepared dense samples of atomic lithium and molecular calcium monohydride at temperatures as low as 1 Kelvin. We have measured the Li + CaH → LiH + Ca chemical reaction, observed in both the accelerated disappearance of CaH in the presence of high densities of lithium, and in the appearance of the LiH molecule.

PACS numbers: 34.50.Lf, 34.50.Cx, 37.10.De

The development of new techniques for producing cold molecules has opened up the field of cold chemistry. Working with cold reactants offers the possibility of unprecedented energy resolution as well as internal state control. This is not only of interested for the detailed study of chemical reactions, but also for the development of new techniques for controlling reactions [1].

In prior work, cold molecules have been employed in nonreactive collision experiments, which have measured cross-sections for inelastic and elastic processes with fine energy resolution [2–6], as well as demonstrating the manipulation of these cross-sections with applied fields [7, 8]. In chemical reaction experiments, cold ion–molecule reactions have been measured at temperatures down to 1 K using supersonic jets and ion traps [9, 10]. Cold neutral chemical reactions have traditionally been observed through the CRESU technique [11–13]; more recently reactions have been observed in samples of ultracold bialkali molecules formed from ultracold atoms, and control of the reaction rate via internal-state preparation has been demonstrated [14].

Here, we describe measurements of the Li + CaH → LiH + Ca reaction at 1 K. The reaction is exothermic, releasing 0.9 eV of energy [15, 16]. The cold reactants are prepared by cryogenic buffer-gas cooling, a technique which should be applicable to a much wider range of chemical species than molecules produced from ultracold atoms [17]. Additionally, cryogenic buffer-gas cooling allows measurements of reactions at temperatures an order of magnitude colder than have been obtained with CRESU, and allows for detection of the reaction products. While 1 Kelvin is in the multiple-partial-wave limit, it allows for the opportunity to control reactions with applied fields and state preparation [18].

We produce cold atomic Li and molecular CaH by cryogenic helium buffer gas cooling [19]. The experiment takes place in a 10 cm cubic copper cell, similar to that described in reference [20]. The cell is cryogenically cooled by a cryogen-free ^{4}He refrigerator, which uses a commercial pulse tube cooler to condense the circulating ^{4}He [21]. The cell temperature is monitored by a ruthenium oxide resistor. The helium density is determined from a room-temperature pressure gauge connected to the cell through a thin tube. We correct for the thermomolecular pressure ratio with the Weber-Schmidt equation [22]. The uncertainty in measured helium densities in this paper is approximately ±20%. Gas-phase Li and CaH are produced by laser ablation of solid targets of 99.9% pure Li and 95% pure CaH_2 with a frequency-doubled Nd:YAG laser.

Li atoms and CaH molecules are detected by laser absorption spectroscopy, as described in reference [23]. Li atoms are detected on the D1 transition at 671 nm [24, 25]. Ground-state CaH molecules are detected on the $B\ ^2\Sigma(v'=0, N'=1, J'=\frac{3}{2}) \leftarrow X\ ^2\Sigma(v''=0, N''=0, J''=\frac{1}{2})$ transition at 634 nm [26, 27]. Typical probe powers are on the order of a few μW, with a beam diameter of a few mm.

Typical buffer gas densities range from 2×10^{15} cm^{-3} to 1×10^{16} cm^{-3}, giving Li diffusion lifetimes from 0.02 s to 0.1 s and CaH diffusion lifetimes from 0.06 s to 0.2 s. We are able to produce lithium and calcium hydride densities as high as $n_{\mathrm{Li}} = 10^{12}$ cm^{-3} and $n_{\mathrm{CaH}} = 10^{8}$ cm^{-3}, with ablation energies of tens of mJ. The translational temperature of the gas is directly measured through spectroscopy of the atomic lithium; under our conditions Doppler broadening is the dominant broadening mechanism. Thermalization with the buffer-gas occurs within 1 ms.

We observe the cold chemical reaction Li + CaH → LiH + Ca through the accelerated disappearance of the reactants and the appearance of the products.

For the reaction products, we do not attempt to observe the Ca produced; this is likely to be impractical due to the large amounts of Ca atoms expected to be produced by the ablation of the CaH_2 target. We detect LiH molecules using laser induced fluorescence (LIF) by exciting them on the $A\ ^1\Sigma(v'=5, J'=1) \leftarrow X\ ^1\Sigma(v''=2, J''=0)$ transition at 401 nm [28, 29]. The LIF signal is observed using a photomultiplier tube (PMT). We use a bandpass filter with high transmission from 350 nm to 390 nm to block scattered light and transmit frequency-shifted LiH LIF from decay to the $X\ ^1\Sigma(v''=0)$ and $(v''=1)$ states, at 362 and 381 nm, respectively [29, 30]. The observed LiH LIF signal is shown in Fig. 1. We note that no LiH signal is observed if the Li or CaH targets

are ablated separately.

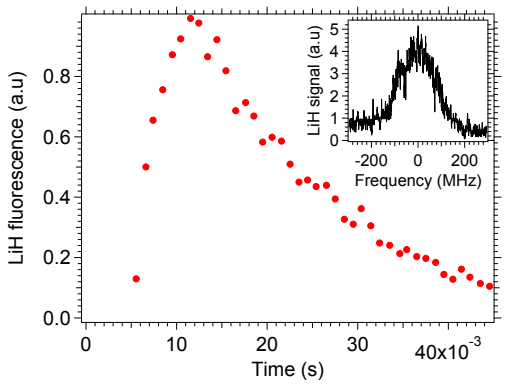

FIG. 1. (Color online) LiH laser-induced-fluorescence, measured at a helium density 6.7×10^{15} cm^{-3}. The inset shows a spectrum of the LiH; the frequency offset is 24922 cm^{-1}. In the graph of LiH fluorescence as a function of time, the Li and CaH are produced by laser ablation at $t = 0$; the PMT measuring fluorescence is gated off until +3 ms to protect it from the ablation flash.

The LiH is expected to be produced at high kinetic energies due to the large energy released in the reaction. Because the reaction occurs within a high-density helium buffer gas, we expect the translational kinetic energy to be cooled on a $\lesssim 100$ μs timescale. This is consistent with the data; from the width of the LIF spectral line in Fig. 1, we measure a translational temperature of 1 K. We expect inelastic rotation-changing collisions to cool the rotational temperature on a similar timescale [31–33]. The resulting concentration of population into the lowest rotational level greatly aids spectroscopic detection. Conversely, we expect that the vibrational levels will relax slowly in collisions with helium, allowing the observation of excited vibrational states [23, 34]. This offers the potential to measure the distribution of vibrational states produced.

We note that initially the LiH signal increases with time, as expected for LiH produced by cold chemical reactions of Li and CaH. At later times, the signal decreases, as the CaH population is depleted and the existing LiH is lost. We note that the observed LiH lifetime in the cell is shorter than the atomic Li diffusion lifetime. This is likely due to vibrational relaxation, as we detect LiH in an excited vibrational state. Population loss can occur from both collisional quenching and radiative decay [23, 35].

Unfortunately — due to uncertainty in the calibration of our laser-induced-fluorescence detection, uncertainty in the distribution of vibrational states of LiH produced, and uncertainty in the amount of LiH produced at early times while the atoms and molecules are hot — we cannot use the LiH signal to accurately determine the reaction rate coefficient. Instead, we use the measured behavior of the reactants. Because the CaH densities are many orders of magnitude lower than those of Li, we expect little change in the atomic lithium density due to the reaction. We measure reaction rates through the accelerated disappearance of CaH.

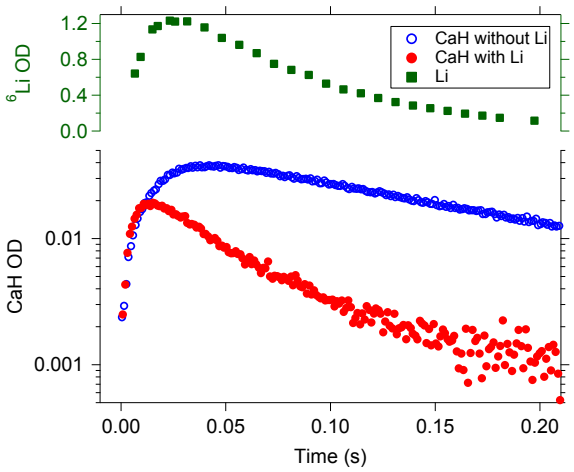

FIG. 2. (Color online) The optical density (OD) of CaH (circles) and Li (squares) as a function of time, as described in the text. The transmission of the probe beam is $T = e^{-\mathrm{OD}}$. CaH behavior is shown both in the presence of Li (filled circles) and without Li (open circles). Data taken at a helium density of 7.3×10^{15} cm^{-3}.

In the absence of Li atoms, the density of CaH decays in time due to diffusion to the cell walls. As seen in Fig. 2, at long times after the ablation this decay is well described by a single exponential, indicating that density distribution is well described by the lowest-order diffusion mode [36]. When Li atoms are introduced into the cell, we observe accelerated loss due to chemical reactions, as shown in Fig. 2. At very early times, when the lithium density in the cell is small, the CaH density is largely unchanged. As the lithium density increases, the loss rate of CaH increases dramatically. At long times after ablation, as the lithium density goes to zero, the CaH decay rate asymptotically approaches the diffusion rate.

We model the CaH population decay from diffusion of CaH molecules to the cell wall and the reaction of CaH molecules with Li atoms. The rate equation for the CaH density $n(x,t)$ may be written as

$$\frac{\partial n(x,t)}{\partial t} = -D\nabla^2 n(x,t) - k n_{Li}(x,t) n(x,t) \qquad (1)$$

where D is the diffusion constant, n_{Li} is Li density, and k is the rate coefficient of Li–CaH reaction [36]. The

boundary conditions are $n(x,t) = 0$ at the cell walls. To extract the Li–CaH reaction rate, we define the function $f(x,t) = n_A(x,t)/n_B(x,t)$, where n_A and n_B are the CaH densities with and without Li in the cell, respectively. If we assume that the spatial distribution of CaH molecules in the cell is not modified by the presence of Li atoms in the cell, we find

$$-\frac{1}{f}\frac{\partial f}{\partial t} = k n_{Li}(x,t) \tag{2}$$

Consequently, we define $-\frac{1}{f}\frac{\partial f}{\partial t}$ as the CaH reaction rate. Because the measured optical density is linearly proportional to the integrated CaH density in the cell, we calculate the reaction rate by taking f to be the ratio of the CaH OD with and without lithium in the cell. The measured CaH reaction rate is shown in Fig. 3, and shows the expected linear dependence on Li optical density.

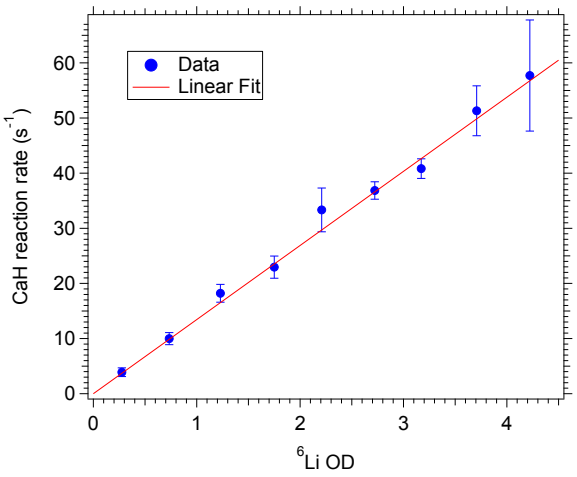

FIG. 3. (Color online) CaH reaction rate, as measured at different ^{6}Li optical densities. Data taken at a helium density of 3.9×10^{15} cm^{-3}, temperatures range from 1.3 K to 1.9 K. Ablation energies varies from 20 mJ to 50 mJ.

To confirm that the accelerated disappearance of CaH is due to the Li + CaH → LiH + Ca reaction, we must rule out all other possible processes.

Inelastic collisions may be ruled out, as we detect CaH in its lowest energy state, and both the Li and CaH are cold. Accelerated hydrodynamic transport to the cell walls due to "stirring" of the buffer-gas by the ablation of Li [37] may be ruled out because it would affect the rate of disappearance of Li as well; no such change in the lithium lifetime with lithium ablation power is observed. Another set of possible processes are reactions with other species produced by laser ablation of the lithium target, such as dust particles, dimers, and clusters. Fortunately, the production of these species should have a strong dependence on the ablation power and helium density [38], and the diffusion lifetime of such species will be different from Li due to their larger mass. We note that the observed CaH reaction rate coefficient is independent of the ablation power, the time after ablation pulse, and the helium density, as shown in Fig. 4. This allows us to rule out CaH reactions with ablation products other than Li. Finally, another possible process is three-body collisions with Li and He; this may be ruled out as the measured reaction rate coefficient is independent of the helium density, as shown in Fig. 4.

To extract the reaction rate coefficient k, we must convert the measured Li OD into a lithium density and account for the inhomogeneous density distribution of Li and CaH in the cell. Approximating our cell volume as a cube, and the density distribution of both Li and CaH by the lowest-order diffusion mode [36, 39], we find

$$k = k_{OD} \cdot \sigma \cdot L \cdot 0.075 \cdot 128 \cdot \pi^{-4} \tag{3}$$

where k_{OD} is the rate coefficient in term of ^{6}Li OD, which is the slope of a plot of CaH reaction rate vs ^{6}Li OD as shown in Fig. 3, σ is Doppler broadened absorption cross-section, and L is the cell length. The factor of 0.075 accounts for the relative isotopic abundance of ^{6}Li [25] and $128 \cdot \pi^{-4}$ corrects for the distribution of Li and CaH in the cell.

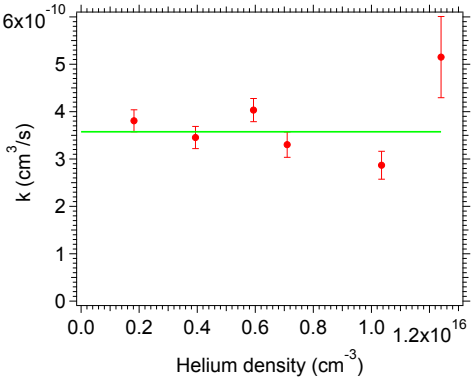

FIG. 4. (Color online) CaH rate coefficient vs helium density. The rate coefficient is independent of helium density as expected for CaH and Li two body reaction.

Unfortunately, imaging the lithium density distribution inside the cell indicates that for the majority of our data, the lowest-order diffusion mode is not a good approximation to the actual density distribution in the cell. We cannot completely correct for the actual density distribution, as our absorption images only provide two-dimension information. The uncertainty in the density distribution is the dominant error in our measurement of the rate coefficient.

Rate coefficients measured at different helium densities are shown in Fig. 4. From this data, we determine a reaction rate coefficient of 3.6×10^{-10} cm^3/s, with a factor of 2 uncertainty.

We compare the two methods of observing the chemical reaction (shown in Fig. 1 and 2). From the disappearance of the CaH, we determine the rate of production of LiH. The LiH signal will depend on both this production rate and the loss rate of the LiH. The shape of the LiH curve is consistent with the CaH data for LiH lifetimes from 0 ms to 11 ms (at a 1-sigma error level). This lifetime — when combined with the expected diffusion lifetime — is consistent with the $X(v''=2)$ state's radiative lifetime of 12 ms [35]. Whether or not collisional relaxation also plays a significant role is not something we were able to conclusively measure.

We also note that the number of LiH $X(v''=2, J''=0)$ molecules detected is roughly one order of magnitude smaller than the number of reacted CaH molecules. This discrepancy may be due to errors in our LIF calibration, or due to the distribution of LiH population over multiple vibrational levels. We note that 4 or 5 different vibrational levels of LiH may be produced in the Li + CaH reaction [15, 16].

In conclusion, we have measured cold chemical reactions of Li and CaH at temperatures from 1 Kelvin to 2 Kelvin. The chemical reaction proceeds with a large rate coefficient, as expected for barrierless reactions [40].

These reactions are a promising starting point for investigating new means of controlling chemical reactions. Tscherbul and Krems predict that reactive collisions between ^2S atoms with $^2\Sigma$ molecules can be controlled by controlling the electron spin state of the reactants [41]. Both ^2S atoms and $^2\Sigma$ molecules have one unpaired electron spin. If the reactants collide in the singlet spin state, the reaction will proceed unimpeded. If the reactants are prepared in the triplet state, the reaction should be strongly suppressed. Evidence of this effect has already been observed by Hummon *et. al.* in magnetic trapping experiments [5]. The effect could be investigated in this system by using optical pumping to prepare both Li and CaH in the maximally stretched spin state (thus ensuring all collisions take place in the triplet state), and measuring the change in the reaction rate coefficient. One concern is that this effect might be obscured by spin-changing collisions between Li and CaH (which would alter the spin states of the reactants). Fortunately, theoretical calculations indicate that the rate coefficient for spin-changing Li–CaH collisions is orders-of-magnitude smaller than the unpolarized reaction rate coefficient [42]. Measurement of this effect will be pursued in future work.

ACKNOWLEDGEMENTS

We gratefully acknowledge experimental assistance from Wade J. Cline and Ryan P. Baker in the design and construction of the cryostat, and from Tian Li in the spectroscopic detection of LiH.

This material is based upon work supported by the National Science Foundation under Grant No. PHY 0900190.

* weinstein@physics.unr.edu; http://www.physics.unr.edu/xap/

[1] R. Krems, B. Friedrich, and W. C. Stwalley, eds., *Cold Molecules: Theory, experiment, applications* (CRC Press; Taylor & Francis Group, 2009).
[2] J. J. Gilijamse, S. Hoekstra, Sebastiaan, Y. T. van de Meerakker, G. C. Groenenboom, and G. Meijer, Science **313**, 1617 (2006).
[3] L. Scharfenberg, J. Klos, P. J. Dagdigian, M. H. Alexander, G. Meijer, and S. Y. T. van de Meerakker, Phys. Chem. Chem. Phys. **12**, 10660 (2010).
[4] K. Maussang, D. Egorov, J. Helton, S. Nguyen, and J. Doyle, Physical Review Letters **94**, 123002 (2004).
[5] M. T. Hummon, T. V. Tscherbul, J. Kłos, H.-I. Lu, E. Tsikata, W. C. Campbell, A. Dalgarno, and J. M. Doyle, Phys. Rev. Lett. **106**, 053201 (2011).
[6] C. D. Ball and F. C. De Lucia, Phys. Rev. Lett. **81**, 305 (1998).
[7] L. P. Parazzoli, N. J. Fitch, P. S. Żuchowski, J. M. Hutson, and H. J. Lewandowski, Phys. Rev. Lett. **106**, 193201 (2011).
[8] B. C. Sawyer, B. K. Stuhl, M. Yeo, T. V. Tscherbul, M. T. Hummon, Y. Xia, J. Klos, D. Patterson, J. M. Doyle, and J. Ye, Phys. Chem. Chem. Phys. **13**, 19059 (2011).
[9] T. Mazely and M. Smith, Chemical Physics Letters **144**, 563 (1988).
[10] S. Willitsch, M. T. Bell, A. D. Gingell, S. R. Procter, and T. P. Softley, Phys. Rev. Lett. **100**, 043203 (2008).
[11] I. R. Sims and I. W. M. Smith, Annual Review of Physical Chemistry **46**, 109 (1995).
[12] I. W. M. Smith, Angewandte Chemie International Edition **45**, 2842 (2006).
[13] J. Daranlot, M. Jorfi, C. Xie, A. Bergeat, M. Costes, P. Caubet, D. Xie, H. Guo, P. Honvault, and K. M. Hickson, Science **334**, 1538 (2011), http://www.sciencemag.org/content/334/6062/1538.full.pdf.
[14] S. Ospelkaus, K.-K. Ni, D. Wang, M. H. G. de Miranda, B. Neyenhuis, G. Quéméner, P. S. Julienne, J. L. Bohn, D. S. Jin, and J. Ye, Science **327**, 853 (2010), http://www.sciencemag.org/content/327/5967/853.full.pdf.
[15] P. Fuentealba and O. Reyes, J. Chem.Phys. **87**, 5338 (1987).
[16] K. P. Huber and G. Herzberg, "NIST Chemistry WebBook," (National Institute of Standards and Technology, 2011) Chap. Constants of Diatomic Molecules, http://webbook.nist.gov.
[17] D. R. Willey, R. L. Crownover, D. N. Bittner, and F. C. D. Lucia, Journal of Chemical Physics **89**, 1923

(1988).
[18] R. V. Krems, Phys. Chem. Chem. Phys. **10**, 4079 (2008).
[19] W. C. Campbell and J. M. Doyle, in *Cold Polar Molecules: Creation and Applications*, edited by R. V. Krems, J. M. Doyle, B. Friedrich, and G. Meijer (CRC, 2009).
[20] M.-J. Lu, K. S. Hardman, J. D. Weinstein, and B. Zygelman, Phys. Rev. A **77**, 060701(R) (2008).
[21] K. S. Hardman, *Closed Cycle Liquid 4He Cryogenic Cooler: Toward controlling chemical reactions*, Master's thesis, University of Nevada, Reno (2011).
[22] T. R. Roberts and S. G. Sydoriak, Physical Review **102**, 304 (1956).
[23] M.-J. Lu and J. D. Weinstein, New Journal of Physics **11**, 055015 (2009).
[24] K. Libbrecht, R. Boyd, P. Willems, T. Gustavson, and D. Kim., Am. J. Phys. **63** (1995).
[25] J. E. Sansonetti, W. C. Martin, and S. L. Young, *Handbook of Basic Atomic Spectroscopic Data* (NIST, 2006) http://physics.nist.gov/PhysRefData/Handbook/.
[26] L.-E. Berg and L. Klynning, Astron. Astrophys. Suppl. **13**, 325 (1974).
[27] L.-E. Berg, K. Ekvall, and S. Kelly, Chemical Physics Letters **257**, 351 (1996).
[28] W. C. Stwalley and W. T. Zemke, Journal of Chemical Physics Reference Data **22**, 87 (1993).
[29] N. Bouloufa, P. Cacciani, R. Vetter, and A. Yiannopoulou, Journal of Molecular Spectroscopy **202**, 37 (2000).
[30] W. T. Zemke and W. C. Stwalley, Journal of Chemical Physics **68**, 4619 (1978).
[31] N. Balakrishnan, G. C. Groenenboom, R. V. Krems, and A. Dalgarno, Journal of Chemical Physics **118**, 7386 (2003).
[32] C. D. Ball and F. C. D. Lucia, Chemical Physics Letters **300**, 227 (1999).
[33] W. H. al Qady, R. C. Forrey, B. H. Yang, P. C. Stancil, and N. Balakrishnan, Phys. Rev. A **84**, 054701 (2011).
[34] W. C. Campbell, G. C. Groenenboom, H.-I. Lu, E. Tsikata, and J. M. Doyle, Physical Review Letters **100**, 083003 (2008).
[35] W. T. Zemke and W. C. Stwalley, The Journal of Chemical Physics **73**, 5584 (1980).
[36] J. B. Hasted, *Physics of Atomic Collisions*, 2nd ed. (American Elsevier, 1972).
[37] D. Patterson and J. M. Doyle, The Journal of Chemical Physics **126**, 154307 (2007).
[38] A. D. Sappey and T. K. Gamble, Applied Physics B: Lasers and Optics **53**, 353 (1991), 10.1007/BF00331827.
[39] M.-J. Lu, V. Singh, and J. D. Weinstein, Phys. Rev. A **79**, 050702 (2009).
[40] J. M. Hutson and P. Soldán, International Reviews in Physical Chemistry **26**, 1 (2007), http://www.tandfonline.com/doi/pdf/10.1080/01442350601084562.
[41] T. V. Tscherbul and R. V. Krems, Phys. Rev. Lett. **97**, 083201 (2006).
[42] T. V. Tscherbul, J. Klos, and A. A. Buchachenko, arXiv , 1106.1492 (2011).